Manuscript Number: HE-D-11-01499R1

Title: Hybrid sulfur cycle flowsheets for hydrogen production using high-temperature gas-cooled reactors

Article Type: Full Length Article

Keywords: Hydrogen production; nuclear heat application; hybrid sulfur cycle; process flowsheet; Aspen Plus; proton exchange membrane electrolyzer; bayonet decomposition reactor

Corresponding Author: Dr. Maximilian B. Gorensek, Ph.D., P.E.

Corresponding Author's Institution: Savannah River National Laboratory

First Author: Maximilian B. Gorensek, Ph.D., P.E.

Order of Authors: Maximilian B. Gorensek, Ph.D., P.E.

Abstract: Two hybrid sulfur (HyS) cycle process flowsheets intended for use with high-temperature gas-cooled reactors (HTGRs) are presented. The flowsheets were developed for the Next Generation Nuclear Plant (NGNP) program, and couple a proton exchange membrane (PEM) electrolyzer for the SO2-depolarized electrolysis step with a silicon carbide bayonet reactor for the high-temperature decomposition step. One presumes an HTGR reactor outlet temperature (ROT) of 950°C, the other 750°C. Performance was improved (over earlier flowsheets) by assuming that use of a more acid-tolerant PEM, like acid-doped poly[2,2'-(m-phenylene)-5,5'-bibenzimidazole] (PBI), instead of Nafion®, would allow higher anolyte acid concentrations. Lower ROT was accommodated by adding a direct contact exchange/quench column upstream from the bayonet reactor and dropping the decomposition pressure. Aspen Plus was used to develop material and energy balances. A net thermal efficiency of 44.0% to 47.6%, higher heating value basis is projected for the 950°C case, dropping to 39.9% for the 750°C case.

Highlights for "Hybrid sulfur cycle flowsheets for hydrogen production using high-temperature gas-cooled reactors"

- Two hybrid sulfur cycle flowsheets are presented that combine a bayonet decomposition reactor with a proton exchange membrane electrolyzer.
- Aspen Plus material and energy balances are provided.
- One flowsheet can be used with a 950°C reactor to make hydrogen at 44.0% to 47.6% net thermal efficiency, HHV basis.
- The other flowsheet can be used with a 750°C reactor to make hydrogen at 38.0% net thermal efficiency, HHV basis.

Hybrid sulfur cycle flowsheets for hydrogen production using high-temperature gas-cooled reactors

Maximilian B. Gorensek*

Process Modeling and Computational Chemistry Section, Savannah River National Laboratory, Aiken, SC 29808 USA

Abstract

Two hybrid sulfur (HyS) cycle process flowsheets intended for use with high-temperature gas-cooled reactors (HTGRs) are presented. The flowsheets were developed for the Next Generation Nuclear Plant (NGNP) program, and couple a proton exchange membrane (PEM) electrolyzer for the SO_2-depolarized electrolysis step with a silicon carbide bayonet reactor for the high-temperature decomposition step. One presumes an HTGR reactor outlet temperature (ROT) of 950°C, the other 750°C. Performance was improved (over earlier flowsheets) by assuming that use of a more acid-tolerant PEM, like acid-doped poly[2,2'-(*m*-phenylene)-5,5'-bibenzimidazole] (PBI), instead of Nafion®, would allow higher anolyte acid concentrations. Lower ROT was accommodated by adding a direct contact exchange/quench column upstream from the bayonet reactor and dropping the decomposition pressure. Aspen Plus was used to develop material and energy balances. A net thermal efficiency of 44.0% to 47.6%, higher heating value basis is projected for the 950°C case, dropping to 39.9% for the 750°C case.

Keywords: Hydrogen production; nuclear heat application; hybrid sulfur cycle; process flowsheet; Aspen Plus; proton exchange membrane electrolyzer; bayonet decomposition reactor

* Tel.: (803) 725-1314; Fax: (803) 725-8829;
E-mail address: maximilian.gorensek@srnl.doe.gov

Acronyms

DOE	US Department of Energy
DOE-NE	DOE Office of Nuclear Energy
HHV	Higher heating value
HTGR	High-temperature gas-cooled reactor
HyS	Hybrid sulfur
IHX	Intermediate heat exchanger
NGNP	Next Generation Nuclear Plant
NHI	Nuclear Hydrogen Initiative
PBI	Poly[2,2'-(*m*-phenylene)-5,5'-bibenzimidazole]
PCU	Power conversion unit
PEM	Proton exchange membrane (alternative definition: polymer electrolyte membrane)
ROT	Reactor outlet temperature (nuclear reactor)
SDE	SO_2-depolarized electrolyzer
SI	Sulfur-iodine
SNL	Sandia National Laboratories
SRNL	Savannah River National Laboratory
USC	University of South Carolina

1

1. Introduction

The HyS cycle is one of the three primary hydrogen production methods that were being developed for the US Department of Energy (DOE) Office of Nuclear Energy (DOE-NE) under the Nuclear Hydrogen Initiative (NHI) [1, 2]. (The other two methods were high-temperature electrolysis and the sulfur-iodine (SI) cycle.) Despite significant technical progress, the NHI was discontinued by DOE in October, 2009 as part of a general reduction in support for hydrogen energy research. Development of the HyS cycle under the NHI had been led by the Savannah River National Laboratory (SRNL) [3], which proposed to couple a PEM-based SO_2-depolarized electrolyzer (SDE) [4] with a bayonet type high temperature sulfuric acid decomposition reactor that had been designed and built by Sandia National Laboratories (SNL) for the SI cycle [5]. A conceptual design for such a process was published previously [6].

Motivation for the NHI was provided by the DOE-NE's NGNP program [7], which seeks to build an HTGR for demonstration purposes to advance commercialization of HTGRs for electricity generation and process heat applications. One of the original purposes of NGNP was to provide a high-temperature heat source for hydrogen production [8]. However, the NGNP program was recently restructured to deemphasize hydrogen generation, and the design was modified to focus on lower temperature operation aimed at other process heat applications [9], such as high temperature steam generation. Nevertheless, several improvements to the HyS process were made in the final days of the NHI that make a strong case for its further development. Two of these are detailed in the following pages.

2. Background/Motivation

The HyS cycle (Figure 1) is one of the simplest, all-fluids thermochemical cycles for splitting water with a high-temperature heat source. Originally patented in 1975 by Brecher and Wu [10], the only element it uses besides hydrogen and oxygen is sulfur, which is cycled between the +4 and +6 oxidation states. HyS comprises two steps: one is the (high-temperature) thermochemical decomposition of sulfuric acid (H_2SO_4) to sulfur dioxide (SO_2), oxygen (O_2), and water;

$$H_2SO_4(aq) \rightarrow H_2O(g) + SO_2(g) + \tfrac{1}{2}O_2(g) \quad (1)$$

the other is the SO_2-depolarized electrolysis of water to H_2SO_4 and hydrogen (H_2).

$$SO_2(aq) + 2H_2O(l) \rightarrow H_2SO_4(aq) + H_2(g)\,,\ E^\circ = -0.156\text{V [11]} \quad (2)$$

It is the electrochemical nature of this second reaction that makes it a hybrid cycle. Researchers at the SRNL and at the University of South Carolina (USC) have successfully used PEM electrolyzers (Figure 2) for the SDE (sulfur oxidation) step, while others at SNL successfully utilized a bayonet-type reactor (Figure 3) for the high-temperature sulfuric acid decomposition (sulfur reduction) step. Coupling these two operations should result in a simple process that has the potential to be more efficient and cost-effective for the massive production of hydrogen than alkaline electrolysis.

The basic concepts of the HyS cycle have already been described in the literature. A comprehensive review has also been published recently [12].

The original plan for NGNP called for an HTGR ROT of at least 1000°C (1273K) [13]. This was initially lowered to 950°C (1223K) [14] and finally to 750°C (1023K) [15] due to concerns about the longevity of the intermediate heat exchanger (IHX). For comparison, the flowsheet published previously [6] assumed an ROT of 945°C (1218K). All else being equal,

lowering the ROT inevitably leads to lower energy efficiency, since the ideal efficiency of water-splitting has a Carnot-type dependence on ROT as shown by Knoche and Funk [16]. Furthermore, a pinch analysis of the bayonet reactor [17] suggested that lowering the ROT below 825°C (1098K) would not result in a practical HyS process due to recuperation limitations within the bayonet itself. These considerations prompted a careful reexamination of the flowsheet, since the 685.8-kJ/mol H_2 energy requirement that was reported earlier [6] for the 945°C (1218K) ROT case corresponded to an HHV efficiency[1] of only 41.7%. For comparison, an alkaline electrolysis process powered by an HTGR power plant could be expected to achieve an HHV efficiency of about 36% [6].

3. Approach

The simplicity of the two key components of this process is an attractive feature that leads to a relatively simple flowsheet. However, there is more to HyS than just these two operations, and integrating them requires some compromises.

Given the choice, the SDE should be maintained at the highest possible conversion (to minimize the recycle of unreacted SO_2) and H_2SO_4 content (to minimize the need for further concentration downstream) for efficiency considerations elsewhere in the process. However, the SDE can not be operated at high conversion because the cell potential depends on the concentration of SO_2 at the anode [11]. Earlier work [6, 19] assumed that the SDE operates at 40% SO_2 utilization, requiring a fairly large recycle stream and leaving a significant SO_2 concentration in the anolyte effluent. Consequently, unreacted SO_2 needs to be recovered and recycled before feeding the sulfuric acid product to the decomposition reactor. More importantly,

[1] The HHV, or higher heating value of H_2 is -286 kJ/mol [18].

the concentration of sulfuric acid in the anolyte is also limited. Higher H_2SO_4 concentration leads to lower SO_2 solubility and higher reversible potential [11]. It can also decrease the conductivity of the PEM separator, especially Nafion®, thereby increasing the cell potential [20]. Since efficient operation of the SDE is favored by more dilute (sulfuric acid) anolyte, the concentration of H_2SO_4 in the anolyte effluent also needs to be increased before it is fed to the bayonet reactor.

The high-temperature decomposition of H_2SO_4 is limited by thermodynamic equilibrium and falls well short of complete conversion. This implies that unreacted H_2SO_4 needs to be recovered and recycled in addition to the SO_2 product having to be separated from the O_2 co-product before it can be fed to the SDE. The high-temperature heat requirement is determined by the opportunity for recuperation within the bayonet. Previous work showed that the required heat input is minimized by operating the reactor at the highest possible temperature and pressure, and at a feed concentration of 80.1 wt% H_2SO_4 [17]. A more concentrated acid feed would actually increase the heating target, while feeding less concentrated acid would cause more water to be vaporized and condensed with incomplete recuperation, thereby consuming more high-temperature heat. Concentrations below 65 wt% H_2SO_4 give heating targets in excess of 400 kJ/mol H_2 which, when combined with the other process heat and power needs, results in a net thermal efficiency comparable to that of alkaline electrolysis. Since the HyS cycle has greater complexity, it will not be more cost-effective than water electrolysis unless it has a significant efficiency advantage. An obvious way to maximize efficiency is to operate the SDE at the highest possible acid concentration without adversely affecting the cell potential.

3.1. High-temperature (950°C ROT) flowsheet

The first modification to the original [6] HyS process was made in an effort to improve the net thermal efficiency at the high temperature end, which was only 41.7%, HHV basis as noted in Section 2. The anolyte acid concentration limitation was removed by assuming the use of an alternative PEM material such as acid-doped PBI instead of Nafion®. The electrical resistivity of acid-doped PBI membranes, which can operate at much higher temperatures than Nafion®, actually decreases with acid concentration [21]. (Such membranes were not actually tested in the SDE at SRNL because HyS development under the NHI was discontinued before they could be.) It was assumed, then, that the SDE uses a PEM capable of operating at 65 wt% H_2SO_4 in the anolyte and at temperatures of 120 to 140°C. (Reversible cell potential increases with acid concentration and temperature [11], so operating at higher temperatures or concentrations than this may be limited by thermodynamic considerations.)

The existing HyS flowsheet [19] was modified to reflect operation of the SDE at 120°C and 65 wt% H_2SO_4 in the anolyte product. SO_2 conversion was also increased from 40% to 50%, and a cell potential of 0.6 V imposed. (SDE operation at 0.6 V and 0.5 A/cm^2 was the development target for SRNL and should be attainable with acid-doped PBI PEMs.) Water flux across the membrane was set to maintain a ratio of 1 mol H_2O/mol H_2 product despite the much lower water content of acid-doped PBI and other PEM alternatives (compared to Nafion®). Since a significant water activity gradient will exist between the cathode and anode, it was assumed that the large driving force for water transport would compensate for the reduced water content of the new PEM material.

Raising the cell temperature allows heat dissipated in the SDE due to overpotentials to be recovered in the acid concentration step downstream. Increasing conversion reduces the quantity

of unreacted SO_2 that has to be removed and recycled. Raising the anolyte product acid concentration from 50 to 65 wt% H_2SO_4 allows the quantity of water that has to be removed in the concentration step (in order to increase the acid concentration of the bayonet reactor feed to 75 wt% H_2SO_4) to be reduced by roughly two-thirds. This means less than half as much energy is needed to achieve the necessary concentration, so nearly all of the heat input can be provided by recuperation from the SDE and the bayonet reactor.

Unfortunately, water recovered in the acid concentration step is needed to absorb SO_2 from the uncondensed product of the bayonet decomposition reactor. Since less water is now available for the O_2/SO_2 separation, a single absorber is no longer sufficient because it would leave too much SO_2 behind in the oxygen product.

The addition of an absorber/stripper combination reduces the SO_2 content of the oxygen co-product to $\leq$ 1 ppm using conventional process equipment and without introducing any new reagents. Water is the solvent; the absorber operates at the pressure of the SDE, while the stripper operates at atmospheric pressure, allowing low-pressure steam or recuperation to provide the necessary boil-up. An SO_2 compressor with atmospheric pressure feed is already being used to recycle unconverted SO_2 recovered from the anolyte product, so the overhead from the stripper can be easily added to the recycle compressor feed.

3.2. Low-temperature (750°C ROT) flowsheet

A second set of modifications was made in an effort to accommodate the decrease in ROT from 950 to 750°C for the NGNP program, leading to a new process flowsheet. An earlier pinch analysis had shown that the minimum high-temperature heat requirement (per unit of H_2 production) for the bayonet reactor increases with decreasing operating temperature (Figure 8 in

reference [17]). This results from the unfavorable shift in equilibrium with lower temperatures as well as from changes in internal recuperation within the bayonet. H_2SO_4 conversion also suffers, leading to larger quantities of unconverted acid that need to be re-concentrated and recycled. To counter-act the effects of operation with a catalyst bed exit temperature below 700°C (as mandated by an ROT of 750°C), the operating pressure of the bayonet was first lowered to 12 bar. This helped minimize the high-temperature heat requirement (e.g. see the 700°C curve in Figure 9 in reference [17]) while recovering at least some of the lost H_2SO_4 conversion. A direct contact exchange/quench column was then placed upstream of the bayonet to take advantage of the favorable vapor-liquid equilibrium for the H_2O-H_2SO_4 system and trap unconverted acid in the liquid phase. This eliminated the unconverted acid recycle stream present in the earlier flowsheet [6, 19]. The concentration of the vacuum column bottoms product was increased from 75 to 90 wt% H_2SO_4 to reduce the amount of water being fed to the bayonet reactor/quench column combination (since every mole of water fed exits the loop in the quench overhead and has to be vaporized using HTGR heat). Finally, the bayonet effluent was cooled by heat exchange with heat sinks elsewhere in the process using a DOWTHERM™ G commercial heat transfer fluid loop before feeding it to the bottom of the direct contact exchange/quench column. This provided a significant source of intermediate temperature heat, while diluting the bayonet feed to a near optimal 76 wt% H_2SO_4. The net effect of these changes was attainment of an acceptable level for the high-temperature heat requirement for the bayonet reactor while providing sufficient recuperation from the decomposition reaction product streams to eliminate the need for any additional heat input to the balance of the flowsheet.

4. Results

Aspen Plus (version 7.1) [22] was used to simulate the flowsheets and determine the performance of individual unit operations. Specific details concerning modeling methodology are available in reference [19]. Aspen Energy Analyzer (version 7.1) [23] was used to determine the performance of the bayonet reactor from a pinch analysis based on Aspen Plus simulation data. The details of that calculation are available in reference [17].

4.1. High-temperature (950°C ROT) flowsheet

The design basis for the 950°C ROT HyS process is summarized below in the first data column in Table 1. Rather than pick a specific production rate to match an assumed NGNP heat/power output, the flowsheet was sized at a nominal 1-kmol/sec production rate. This allows all material (molar, mass, and volumetric) and energy (heat and work) flow rates to be multiplied by the actual hydrogen production rate (in kmol/sec) to determine their values for a given application. Note that a 950°C ROT implies hot helium is supplied to the bayonet reactor at 900°C due to an assumed 50°C temperature drop across the IHX. Furthermore, the peak temperature of H_2SO_4 decomposition, which occurs inside the tip of the bayonet (at the outlet of the catalyst bed) is 875°C due to an assumed minimum temperature difference of 25°C between the helium heat transfer medium and the process fluid. Figure 4 illustrates the heat transfer mechanism between the nuclear heat source and the bayonet reactor. The power conversion efficiency of 48%, which assumes that the source of electricity is a power conversion unit (PCU) driven by a 950°C ROT HTGR, is consistent with published projections for NGNP [24]. This PCU could be driven by the same HTGR as the HyS process, or by a separate, electric power HTGR.

The 950°C ROT HyS flowsheet is shown in Figure 5. The stream summary is presented in Table 2. Figure 6 details the heat exchanger network used to preheat the vacuum column feed; fresh sulfuric acid feed is preheated by interchange with the anolyte and catholyte streams, while recycled unconverted acid is preheated by interchange with the bayonet vapor product stream.

The details of the HyS flowsheet are described at length in an earlier paper [6]. The flowsheet in Figure 5 differs from the earlier flowsheet in the following respects: higher SO_2 conversion in the SDE, EL-01 (50 instead of 40%); higher anolyte acid concentration (65 instead of 50 wt% H_2SO_4); higher SDE operating temperature (120 instead of 100°C); detailed heat exchange network (EX-01 through EX-05) with realistic pressure drops (instead of simple stream heaters and coolers connected by heat streams); rigorous vacuum ejector design (instead of fixed entrainment ratio); the overhead product from the original SO_2 absorber, TO-02 is treated in a new absorber/stripper combination (TO-03 and TO-04).

An energy balance was developed from the simulation results. This is presented in the first energy utilization summary, Table 3. Included are the duties and power requirements for all heat exchangers, compressors, pumps, and other energy consumers. Heating and cooling curves were generated using Aspen Plus for all process streams undergoing heat exchange and checked for feasibility. No temperature cross-over was detected; adequate temperature differences were maintained for counter-current heat exchange.

The minimum high-temperature heat requirement for the bayonet reactor was determined from a pinch analysis following the methodology described in reference [17]. The heating (annular flow in) and cooling (center flow out) curves are shown in Figure 7, while the utility composite curve, which demonstrates the operating limits for the secondary helium coolant, is provided as Figure 8.

As shown in Table 3, the net energy efficiency of the 950°C ROT HyS flowsheet is 44.0%, HHV basis if no suitable waste heat source is available, and 47.6%, HHV basis if waste heat from elsewhere in the plant can be exploited to make low-pressure steam. (For comparison, alkaline electrolysis could be expected to achieve 38.6% HHV efficiency when coupled with a PCU operating at 48% conversion efficiency.) This increase (from 41.7%) is attributable to the combined effects of the higher NGNP PCU conversion efficiency (48% instead of 45%), the increase in anolyte acid concentration (from 50 to 65 wt% H_2SO_4) assumed to be attainable with an acid-tolerant PEM, and the increase in SDE SO_2 conversion (from 40 to 50%). It should be noted that the energy required to provide cooling water is not included in this efficiency calculation since the actual amount depends on the type of cooling water system used and is not expected to have a major impact.

4.2. Low-temperature (750°C ROT) flowsheet

The design basis for the 750°C ROT HyS process is summarized below in the second data column in Table 1. As is the case for the 950°C ROT version, the flowsheet was sized at a nominal 1-kmol/sec production rate, allowing the values of all material (molar, mass, and volumetric) and energy (heat and work) flow rates for a given application to be determined by simply multiplying the tabulated value by the actual hydrogen production rate (in kmol/sec). Note that a 750°C ROT implies hot helium is supplied to the bayonet reactor at 700°C due to an assumed 50°C temperature drop across the IHX. An additional 25°C drop between the helium heat transfer medium and the process fluid results in a 675°C peak temperature of H_2SO_4 decomposition inside the tip of the bayonet (at the outlet of the catalyst bed). Heat transfer follows the same path as in Figure 4; the only difference is that the stream temperatures are

200°C lower. The power conversion efficiency of 45% assumes that electricity is provided by a 750°C ROT HTGR PCU and is consistent with efficiency projections for NGNP [24]. This PCU could be driven by the same HTGR as the HyS process, or by a separate, electric power HTGR.

The 750°C ROT HyS flowsheet is shown in Figure 9 and the corresponding stream summary is presented in Table 4. Besides the lower bayonet reactor operating temperature and pressure, this flowsheet differs from that in Figure 5 by the addition of a quench column/direct contact exchanger (new TO-02) and elimination of the unconverted acid stream that was recycled to the vacuum column (TO-01). The concentration of the vacuum column bottoms is also increased from 75 to 90 wt% H_2SO_4. Another difference is the addition of the DOWTHERM™ G heat transfer fluid loop, which recovers intermediate temperature heat from the bayonet reactor product in heat exchangers HX-01 and HX-02 as well as the quench column (TO-02) condenser, and uses it to heat the vacuum column (TO-01) and SO_2 stripper (TO-05) reboilers as well as the steam generator (SG-01) for the vacuum ejectors. As a result, no external steam heat source is needed; all of the necessary heat is provided by the HTGR heat source through the bayonet reactor. Finally, the addition of some and removal of other unit operations resulted in changes in many stream and equipment identification numbers (e.g. TO-03, TO-04, and TO-05 were changed to TO-04, TO-05, and TO-06, respectively).

An energy balance was developed from the simulation results. This is presented in the second energy utilization summary (Table 5). Included are the duties and power requirements for all heat exchangers, compressors, pumps, and other energy consumers. Heating and cooling curves were generated using Aspen Plus for all process streams undergoing heat exchange and checked for feasibility. No temperature cross-over was detected; adequate temperature differences were maintained for counter-current heat exchange.

The minimum high-temperature heat requirement for the bayonet reactor was determined from a pinch analysis following the methodology described in reference [17]. The heating (annular flow in) and cooling (center flow out) curves are shown in Figure 10, while the utility composite curve, which demonstrates the operating limits for the secondary helium coolant, is provided as Figure 11.

As shown in Table 5, the net energy efficiency of the 750°C ROT HyS flowsheet is 39.9%, HHV basis. (Alkaline electrolysis coupled with a PCU operating at 45% conversion efficiency would have an HHV efficiency of 36.2% in comparison.) This is about 1 percentage point lower than expected, based on the drop in energy efficiency for the NGNP PCU (from 48 to 45%) when lowering the ROT from 950 to 750°C. The most likely cause is the significantly increased high-temperature heat requirement for the bayonet reactor, RX-01, (428.3 instead of 340.2 kJ/mol SO_2) which implies less efficient utilization. It should be noted again that this number does not include the energy required to provide cooling water. However, the actual power consumption depends on the type of cooling water system used and is not expected to have a significant impact on efficiency.

5. Discussion

The two new HyS flowsheets presented in Section 4 are projected to achieve significantly higher energy efficiency than alkaline electrolysis coupled with nuclear power. With the exception of the SDE and the bayonet reactor, only proven, well-understood process technology is used that can be accurately characterized with process models. Furthermore, development of the SDE and the bayonet has advanced to the point where their performance targets appear to be attainable. This gives confidence in the validity of the predicted performance for the HyS cycle.

The design of the 750°C ROT flowsheet represents a departure from previous design philosophy in several respects. The pressure differential between the secondary helium coolant and the process fluid, for example, had always been kept to a minimum in order to allow the smallest possible wall thickness for good heat transfer. Given the 40- to 90-bar secondary helium coolant pressure range of the various HTGR options being considered for NGNP, this meant the bayonet would be operated at 40- to 90-bar pressures as well. Lowering the ROT, however, forced a reconsideration of this convention because of the shift in equilibrium conversion. The combination of low temperature and high pressure would have had too negative an impact on the high-temperature (endothermic) decomposition reaction in the bayonet. Moreover, an earlier pinch analysis of the bayonet showed that for ROT below 875°C, the high-temperature heat requirement was minimized by operating at the lowest possible pressure [17]. With that in mind, the process pressure was dropped to 12 bar, which was typical for older sulfuric acid decomposition process designs (e.g. Öztürk et al. [25]). Under the bayonet concept, the high pressure (40-90 bar, depending on the NGNP heat source design) would be on the outside (helium side), putting the silicon carbide walls in compression, for which they should be well-suited. Contamination of high-pressure helium with low-pressure sulfuric acid in the event of a leak or failed seal would also be rendered highly unlikely. Consequently, there shouldn't be any real barrier to operating the bayonet reactor at a significantly lower pressure than the helium heat transfer medium.

The direct contact exchange/quench column is another departure from previous design philosophy. Boiling sulfuric acid is highly corrosive, especially at temperatures in excess of 100-150°C, so any operation that entailed such conditions had been eschewed. However, the H_2SO_4-SO_3-H_2O vapor-liquid equilibrium is highly favorable for trapping unreacted H_2SO_4 and SO_3 in

the liquid phase, and it was necessary to take advantage of this in order to overcome the lower conversion resulting from lower temperature operation. Consequently, the temperature at the bottom of the vacuum column was increased by about 50°C and a quench column was added that handles concentrated sulfuric acid in the 230-260°C range. Suitable materials of construction will need to be identified to withstand this severe service.

Assuming that a sulfuric acid decomposition catalyst active in the 550-675°C range can be developed, this design is a viable option for a HyS cycle process driven by an advanced nuclear reactor heat source operating at 750°C ROT. The projected 39.9% HHV efficiency is significantly better than that for alkaline electrolysis at 36.2%.

6. Conclusions

A HyS cycle process was developed for the massive production of hydrogen from nuclear energy as part of the NGNP program under the NHI. It uses a PEM SDE for the low-temperature, electrochemical reaction step and a novel bayonet reactor for the high-temperature decomposition step. An early version previously published that assumed an HTGR ROT of 945°C was projected to have a net thermal efficiency of 41.7%, HHV basis. Subsequent changes in the NGNP program led to the need to accommodate significantly lower decomposition temperatures. Several improvements to the process resulted from this effort.

If the SDE is operated at 65 wt% H_2SO_4 and the SO_2 conversion is increased to 50% by using a PEM material that does not rely on high water content for its conductivity (such as acid-doped PBI) instead of Nafion®, Aspen Plus flowsheet simulation indicates that all of the heat needed to concentrate the bayonet reactor feed can be provided by recuperation from the SDE and from the bayonet product stream. However, the SO_2/O_2 separation can no longer be achieved

by selective SO_2 absorption into the recycled water and acid using a single absorber column. The addition of an absorber/stripper combination provides the necessary separation with a minimal low-quality heat input. Net thermal efficiencies of 44.0% to 47.6%, HHV basis have been projected if the HTGR ROT is 950°C.

For the 750°C ROT case, the lower decomposition temperature was accommodated by dropping the bayonet pressure to 12 bar, raising the bayonet feed and outlet temperatures, adding a direct contact exchange/quench column upstream, and increasing the vacuum column bottoms concentration to 90 wt% H_2SO_4. Although the minimum heating requirement for the bayonet increased significantly, this was offset by an increase in the opportunity for heat recuperation from the bayonet product that eliminated the need for any additional heat input for acid concentration. A net thermal efficiency of 39.9%, HHV basis is projected for a 750°C HTGR ROT.

Acknowledgements

The author wishes to acknowledge the financial support of DOE-NE provided through Idaho National Laboratory MPO 94714 (Battelle Energy Alliance, LLC) under direction from Mr. M.W. "Mike" Patterson, as well as the encouragement of Dr. William A. Summers, who led SRNL's HyS development effort under the NHI. Helpful interactions with Mr. Charles O. Bolthrunis (Shaw Stone & Webster), Prof. John W. Weidner (USC), and Dr. Edward J. Lahoda (Westinghouse Electric Co.) are also gratefully acknowledged. SRNL is operated for the DOE's Office of Environmental Management by Savannah River Nuclear Solutions, LLC under contract number DE-A C09-08SR22470.

References

[1] Sink CJ. An Overview of the U.S. Department of Energy's Research and Development Program on Hydrogen Production Using Nuclear Energy. *Presentation, AIChE Spring National Meeting, Orlando, FL, United States, April 23-27, 2006.* Available at: http://www.aiche-ned.org/conferences/aiche2006spring/session_51/AICHE2006spring-51b-Sink.pdf. Accessed May 24, 2011.

[2] US Department of Energy, US Department of Transportation. Hydrogen Posture Plan: An Integrated Research, Development and Demonstration Plan. December 2006; Available at: http://www.hydrogen.energy.gov/pdfs/hydrogen_posture_plan_dec06.pdf. Accessed May 24, 2011.

[3] Summers WA. Hybrid Sulfur Thermochemical Cycle. *2009 DOE Hydrogen Program and Vehicle Technologies Program Annual Merit Review and Peer Evaluation Meeting, Arlington, VA, United States, May 18–22, 2009.* Available at: http://www.hydrogen.energy.gov/pdfs/review09/pd_13_summers.pdf. Accessed May 24, 2011.

[4] Colon-Mercado HR, Elvington MC, Steimke JL, Steeper TJ, Herman DT, Gorensek MB, et al. Recent Advances in the Development of the Hybrid Sulfur Process for Hydrogen Production. *Nuclear Energy and the Environment.*ACS Symposium Series Vol 1046: American Chemical Society; 2010:141-154.

[5] Moore RC, Gelbard F, Parma EJ, Vernon ME, Lenard RX, Pickard PS. A Laboratory-Scale Sulfuric Acid Decomposition Apparatus for Use in Hydrogen Production Cycles. *Proceedings: International Topical Meeting on Safety and Technology of Nuclear Hydrogen Production, Control, and Management , Boston, MA, United States, June 24-28, 2007.* 2007:161-166.

[6] Gorensek MB, Summers WA. Hybrid sulfur flowsheets using PEM electrolysis and a bayonet decomposition reactor. *International Journal of Hydrogen Energy.* 2009;34(9):4097-4114.

[7] *Review of DOE'S Nuclear Energy Research and Development Program*. Washington, DC: National Research Council; 2008.

[8] Public Law 109-58 - Energy Policy Act of 2005, §Title VI - Nuclear Matters, Subtitle C - Next Generation Nuclear Plant Project. 109th United States Congress. August 8, 2005.

[9] US Department of Energy, Office of Nuclear Energy. Next Generation Nuclear Plant Demonstration Project. February 15, 2011; Available at: http://www.ne.doe.gov/pdfFiles/factSheets/2012_NGNP_Factsheet_final.pdf. Accessed May 24, 2011.

[10] Brecher LE, Wu CK; Westinghouse Electric Corp., assignee. Electrolytic decomposition of water. US patent 3888750. June 10, 1975.

[11] Gorensek MB, Staser JA, Stanford TG, Weidner JW. A thermodynamic analysis of the SO_2/H_2SO_4 system in SO_2-depolarized electrolysis. *International Journal of Hydrogen Energy.* 2009;34(15):6089-6095.

[12] Gorensek MB, Summers WA. The hybrid sulfur cycle. In: Yan XL, Hino R, eds. *Nuclear Hydrogen Production Handbook.* Boca Raton, FL: CRC Press; 2011:499-545.

[13] Southworth FH, MacDonald PE, Harrell DJ, Shaber EL, Park CV, Holbrook MR, et al. The Next Generation Nuclear Plant (NGNP) Project. Proceedings of Global 2003, Atoms

for Prosperity: Updating Eisenhower's Global Vision of Nuclear Energy; November 16 – 20, 2003; New Orleans, LA.

[14] Burchell T, Bratton RL, Wright RN, Wright J. *Next Generation Nuclear Plant Materials Research and Development Program Plan.* Idaho National Laboratory; INL/EXT-06-11701, Rev. 4. September 2007.

[15] Collins JW. *NGNP Risk Management through Assessing Technology Readiness Status.* Idaho National Laboratory; INL/EXT-10-19197. August 2010.

[16] Knoche KF, Funk JE. Entropy production, efficiency, and economics in the thermochemical generation of synthetic fuels: I. The hybrid sulfuric acid process. *International Journal of Hydrogen Energy.* 1977;2(4):377-385.

[17] Gorensek MB, Edwards TB. Energy Efficiency Limits for a Recuperative Bayonet Sulfuric Acid Decomposition Reactor for Sulfur Cycle Thermochemical Hydrogen Production. *Industrial & Engineering Chemistry Research.* 2009;48(15):7232-7245.

[18] *The Hydrogen Economy: Opportunities, Costs, Barriers, and R&D Needs*. Washington, DC: National Academy of Engineering (NAE); 2004.

[19] Gorensek MB, Summers WA, Bolthrunis CO, Lahoda EJ, Allen DT, Greyvenstein R. *Hybrid Sulfur Process Reference Design and Cost Analysis.* Savannah River National Laboratory; SRNL-L1200-2008-00002. June 12, 2009.

[20] Staser JA, Gorensek MB, Weidner JW. Quantifying Individual Potential Contributions of the Hybrid Sulfur Electrolyzer. *Journal of The Electrochemical Society.* 2010;157(6):B952-B958.

[21] Wainright JS, Wang JT, Weng D, Savinell RF, Litt M. Acid-Doped Polybenzimidazoles: A New Polymer Electrolyte. *Journal of The Electrochemical Society.* 1995;142(7):L121-L123.

[22] *Aspen Plus* [computer program]. Version 7.1 (23.0). Burlington, MA, United States: Aspen Technology, Inc.; 1981-2009.

[23] *Aspen Energy Analyzer* [computer program]. Version 7.1 (23.0). Burlington, MA, United States: Aspen Technology, Inc.; 1995-2009.

[24] McKellar MG. *An Analysis of the Effect of Reactor Outlet Temperature of a High Temperature Reactor on Electric Power Generation, Hydrogen Production, and Process Heat*. Idaho National Laboratory; TEV- 981. September 14, 2010.

[25] Öztürk IT, Hammache A, Bilgen E. An improved process for H_2SO_4 decomposition step of the sulfur-iodine cycle. *Energy Conversion and Management.* 1995;36(1):11-21.

List of Figure Captions

Figure 1 The hybrid sulfur (HyS) cycle.

Figure 2 SRNL PEM SO_2-depolarized electrolyzer (SDE) schematic. The SRNL design features a recirculating anolyte saturated with dissolved SO_2.

Figure 3 SNL high-temperature bayonet H_2SO_4 decomposer schematic. Insulated base where fluid connections are made remains cool. Silicon carbide material of construction can withstand boiling sulfuric acid at high temperatures.

Figure 4 Schematic diagram of heat transfer from nuclear heat source to bayonet reactor.

Figure 5 950°C ROT HyS process flowsheet.

Figure 6 Recuperation detail for 950°C ROT HyS process flowsheet.

Figure 7 Pinch diagram for RX-01 Bayonet Reactor in Figure 5 (950°C ROT).

Figure 8 Hot He utility composite curve for RX-01 Bayonet Reactor in Figure 5 (950°C ROT).

Figure 9 750°C ROT HyS process flowsheet.

Figure 10 Pinch diagram for RX-01 Bayonet Reactor in Figure 9 (750°C ROT).

458 Figure 11 Hot He utility composite curve for RX-01 Bayonet Reactor in Figure 9 (750°C ROT).

459

List of Table Captions

Figure 1

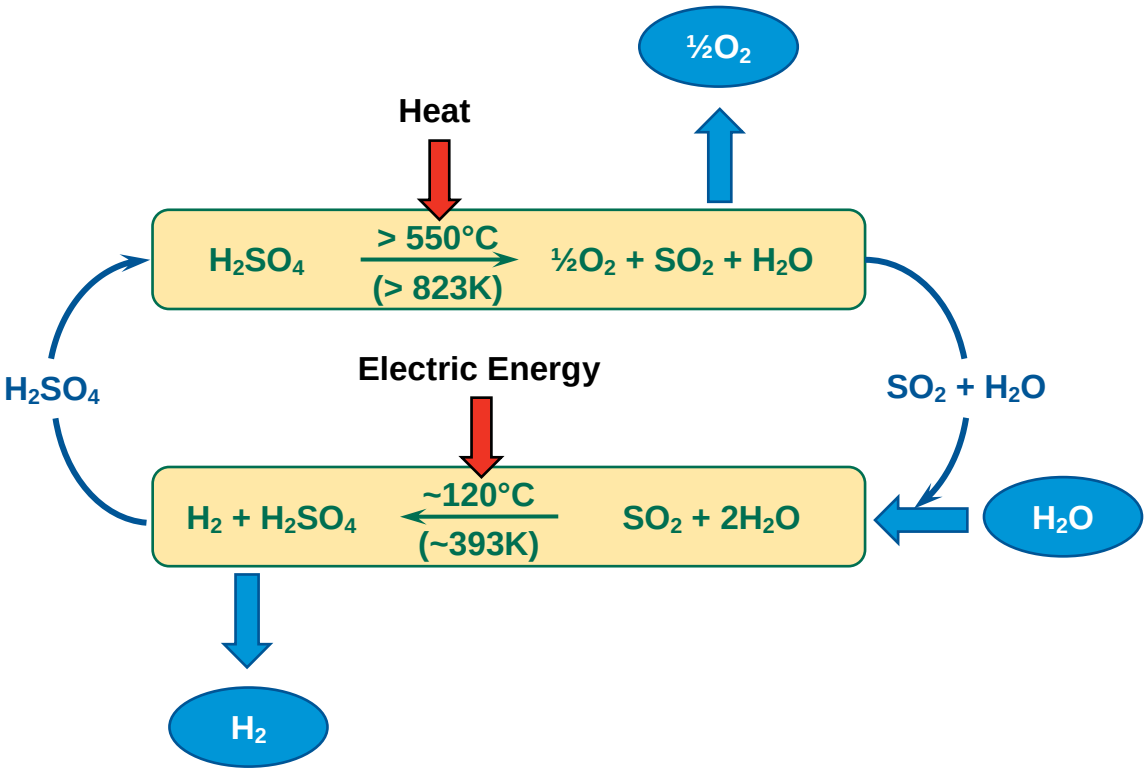

Figure 1

Figure 2

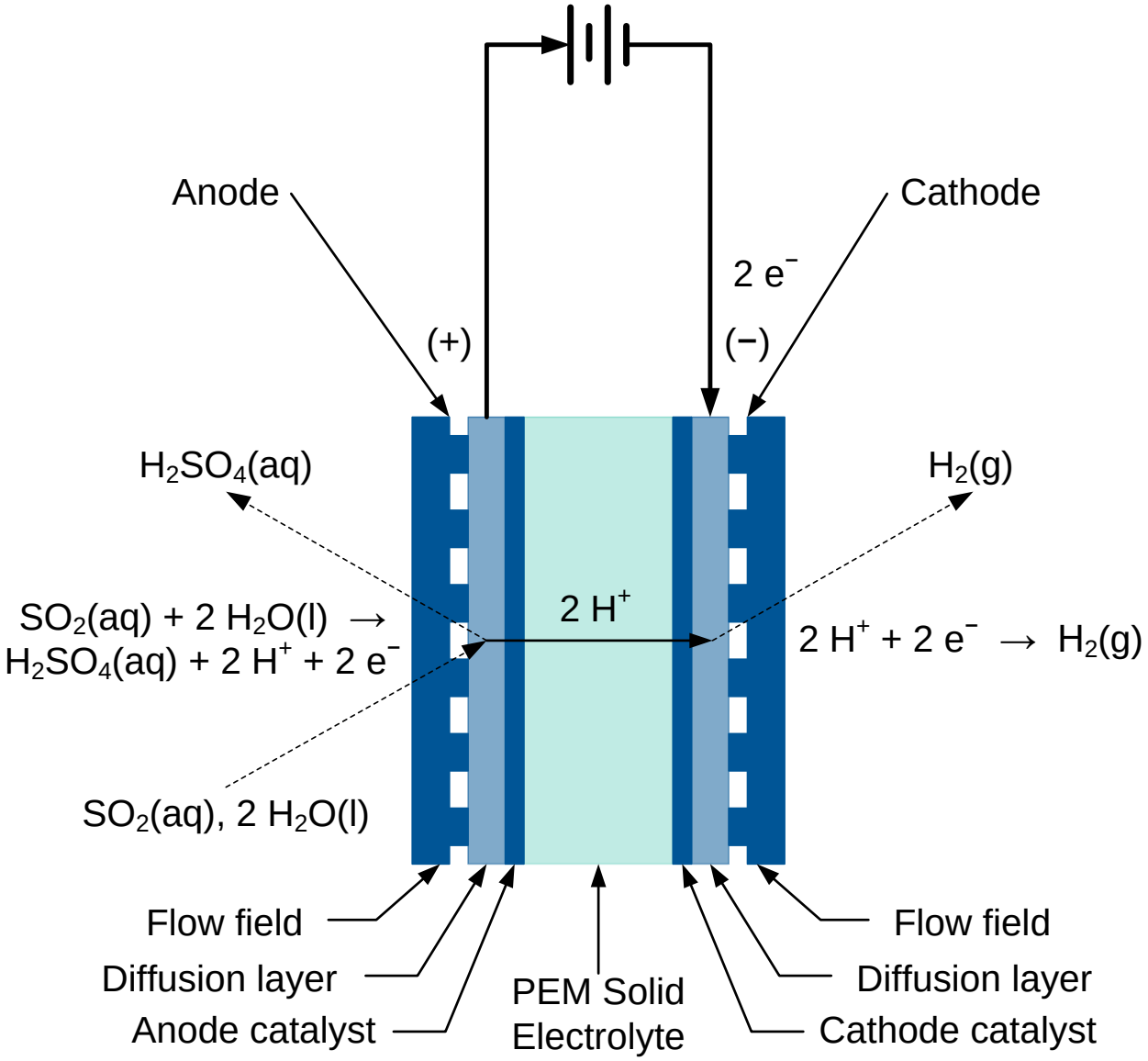

Figure 2

Figure 3

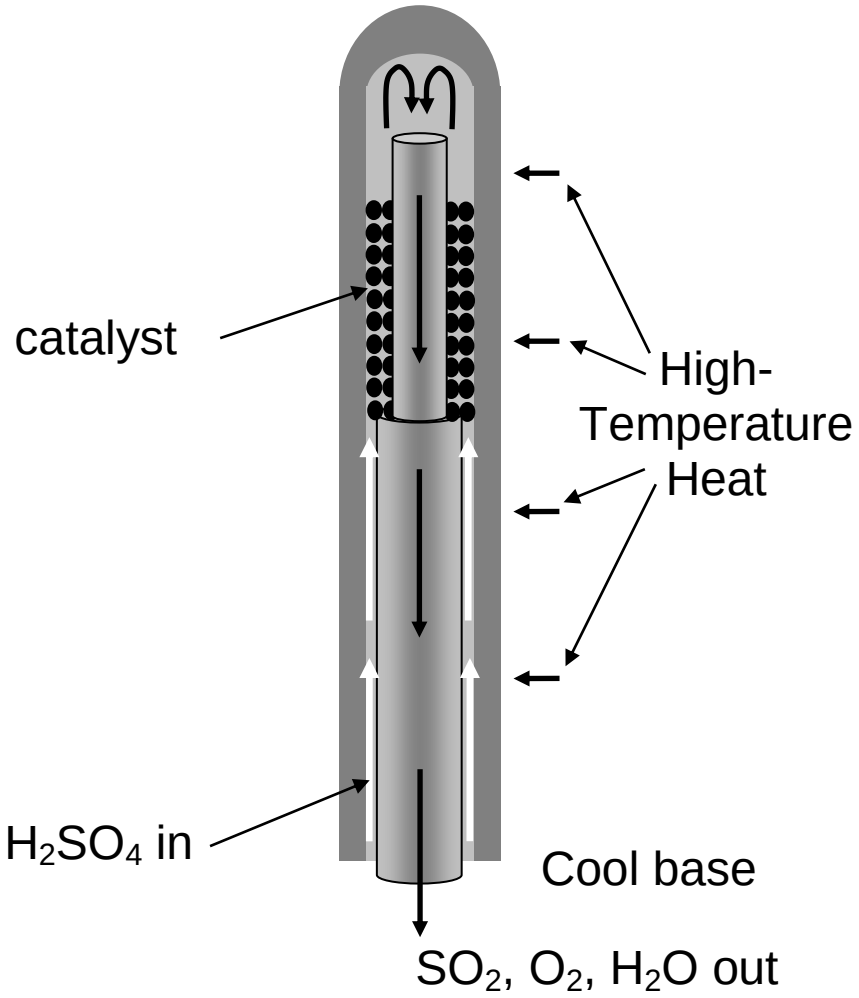

Figure 3

Figure 4

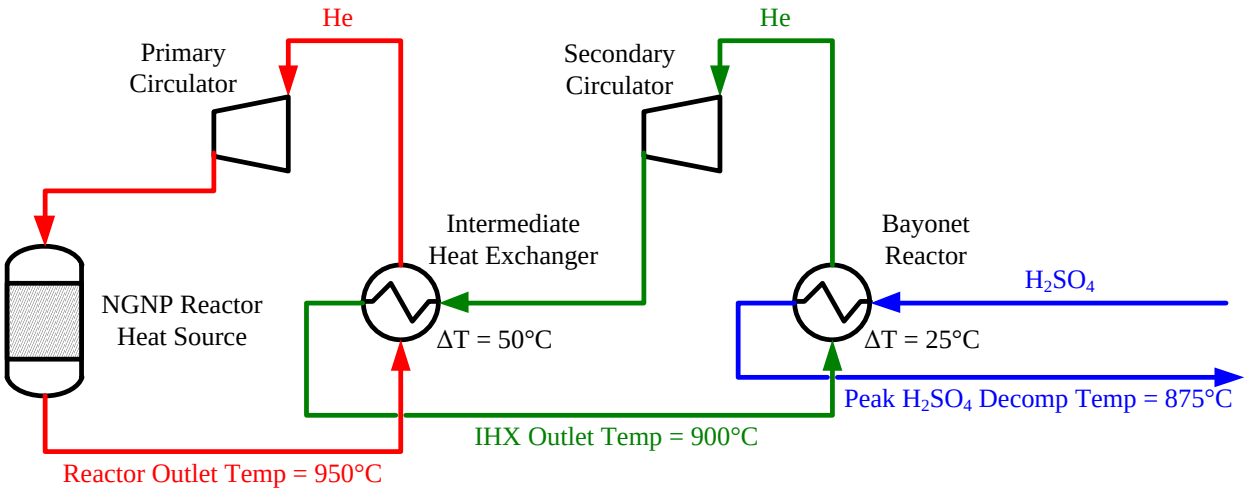

Figure 4

Figure 5

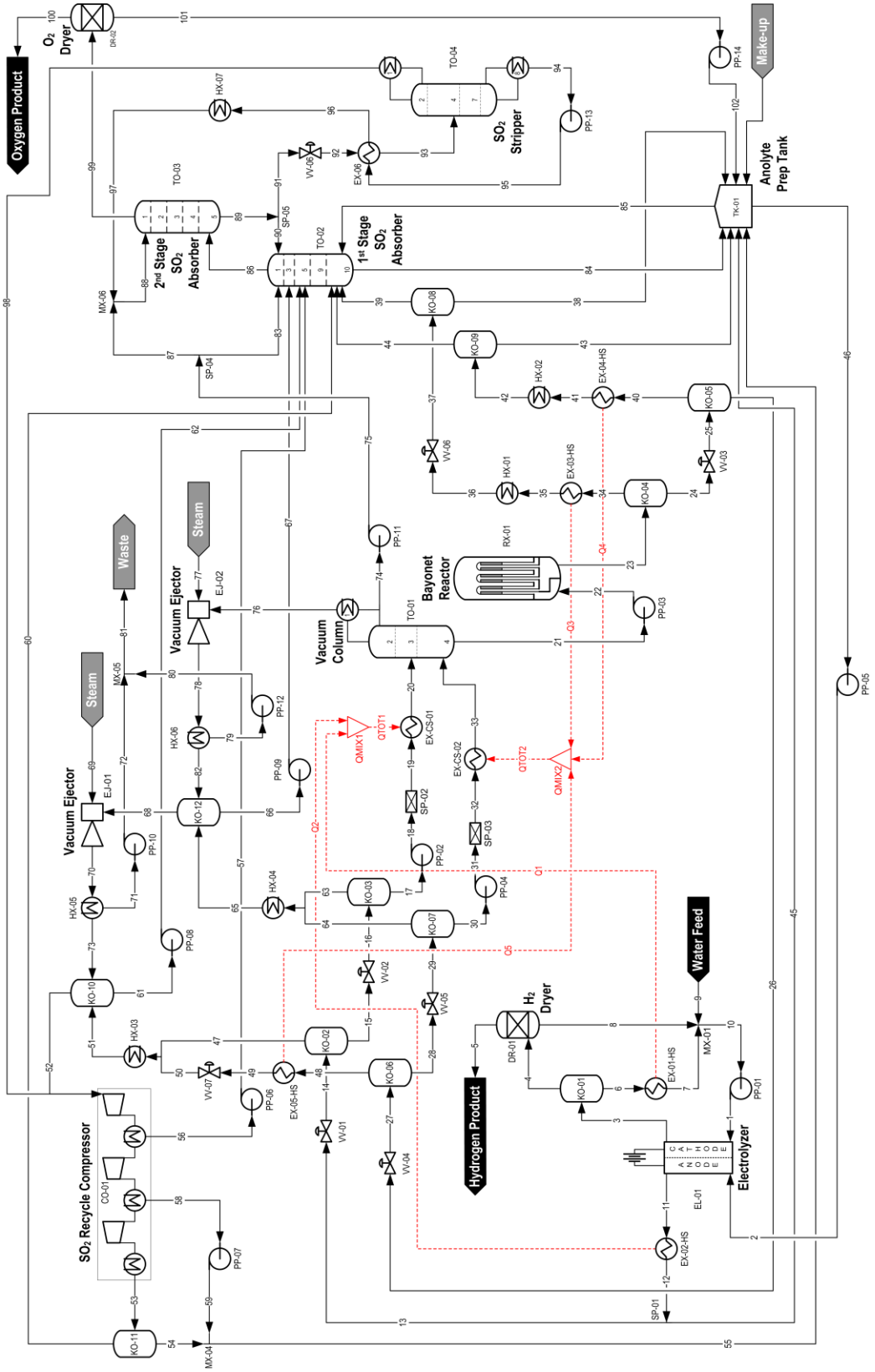

Figure 5

Figure 6

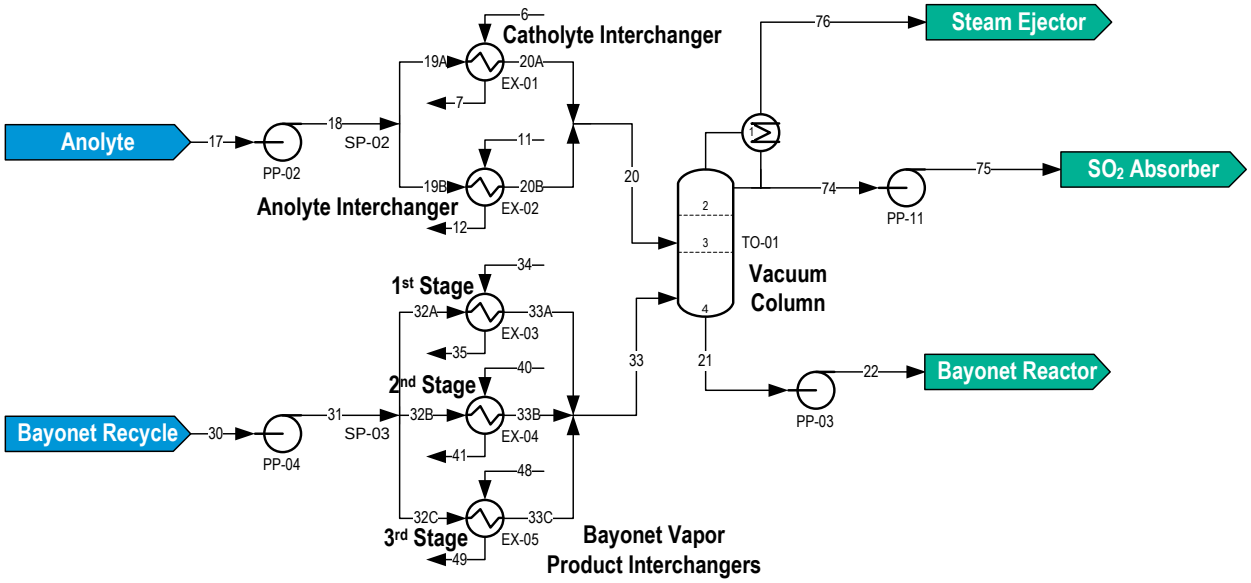

Figure 6

Figure 7

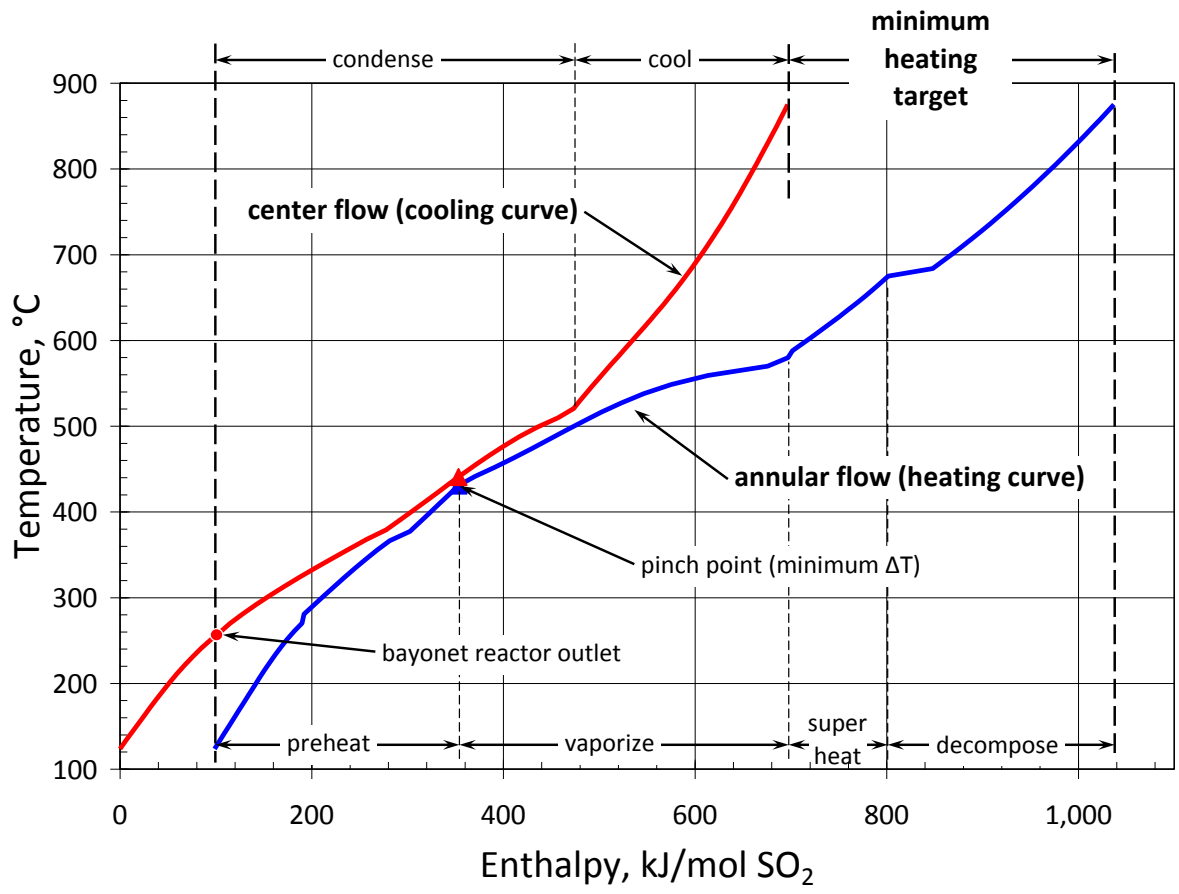

Figure 7

Figure 8

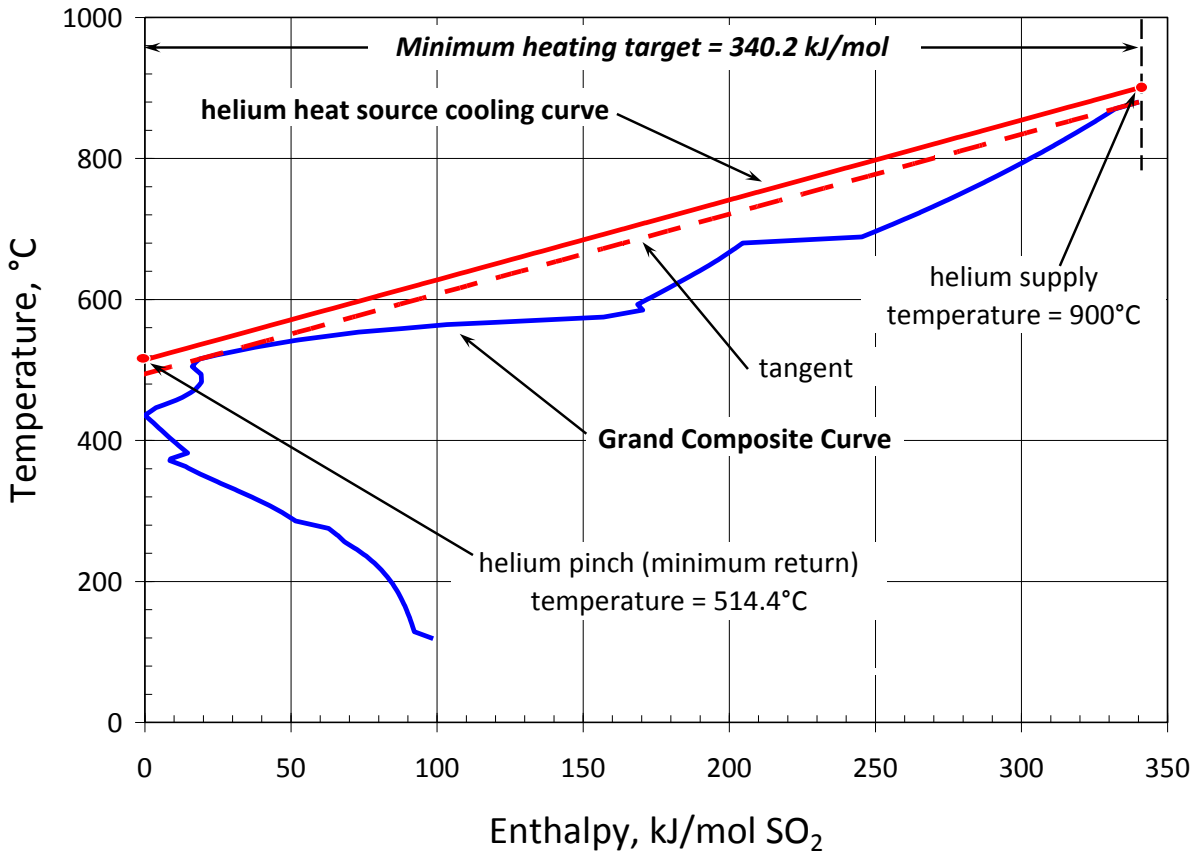

Figure 8

Figure 9

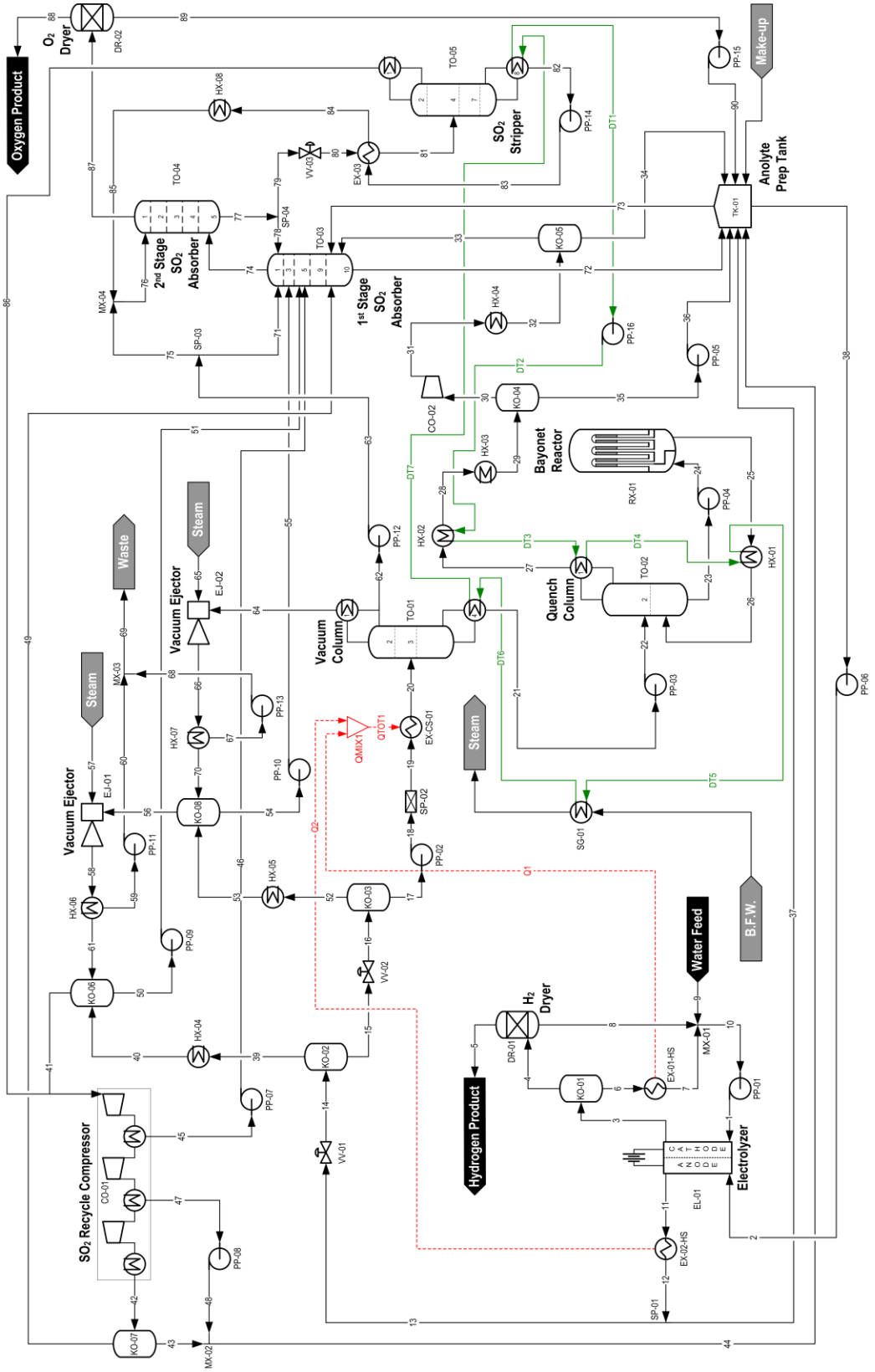

Figure 9

Figure 10

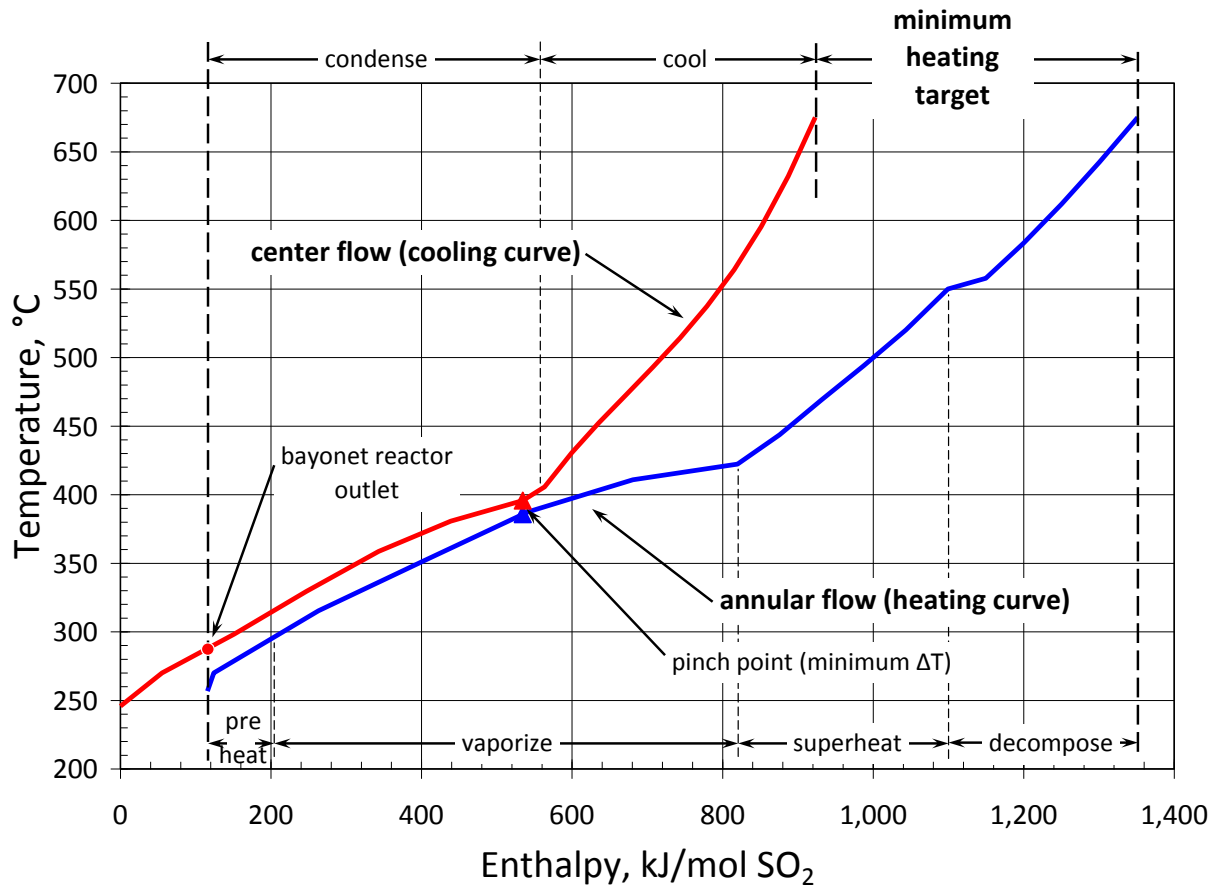

Figure 10

Figure 11

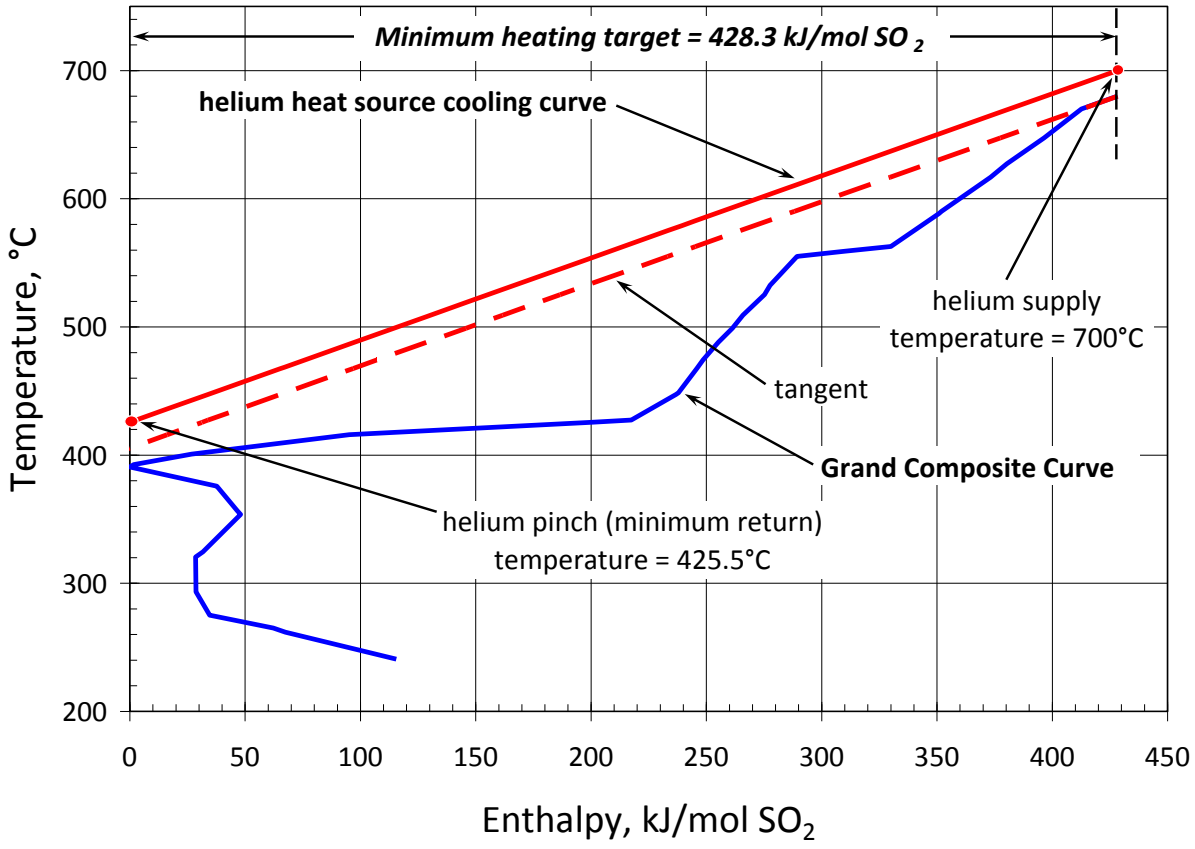

Figure 11

Table 1 Design bases for the 950°C and 750°C ROT HyS process flowsheets.

	950°C ROT Case		750°C ROT Case	
Nominal Hydrogen Production Rate	1	kmol/sec	1	kmol/sec
Hydrogen Product Temperature	48	°C	48	°C
Hydrogen Product Pressure	20	bar	20	bar
Oxygen Co-product Production Rate	0.5	kmol/sec	0.5	kmol/sec
Oxygen Co-product Temperature	48	°C	48	°C
Oxygen Co-product Pressure	20	bar	20	bar
HyS SDE (EL-01) Operating Assumptions				
Operating Temperature	120	°C	120	°C
Operating Pressure	22	bar	22	bar
Operating Potential	0.6	V	0.6	V
SO_2 Concentration in Anolyte Feed	11.8	wt%	11.8	wt%
Acid Product Concentration (Anode)	65	wt%	65	wt%
Conversion (per pass)	50	%	50	%
Cathode Pressure Drop	1	bar	1	bar
Water-swept Cathode				
Water Flux (Cathode to Anode)	1	kmol/sec	1	kmol/sec
Anode Pressure Drop	1	bar	1	bar
Bayonet Reactor (RX-01) Operating Assumptions				
Feed Pressure	86	bar	12.7	bar
Pressure Drop	2	bar	1	bar
Feed Concentration (Quench Column)	N/A		90	wt%
Feed Concentration (Bayonet Reactor)	75	wt%	76.1	wt%
Catalyst Bed Inlet Temperature	675	°C	550	°C
Catalyst Bed Exit Temperature	875	°C	675	°C
Minimum ΔT (Helium to Process)	25	°C	25	°C
Minimum ΔT (Internal Recuperation)	10	°C	10	°C
Equilibrium Attained in Catalyst Bed				
HTGR Operating Assumptions				
Reactor Outlet Temperature	950	°C	750	°C
He Coolant Supply Temperature	900	°C	700	°C
Vacuum Column (TO-01) Operating Conditions				
Overhead Pressure	0.11	bar	0.11	bar
Condenser Temperature	44.1	°C	44.6	°C
Bottoms H_2SO_4 Concentration	75	wt%	90	wt%
Column Pressure Drop	0.02	bar	0.02	bar
Quench Column Operating Conditions	N/A		(TO-02)	

Overhead Pressure		11.1 bar
Condenser Temperature		235 °C
1st Stage SO_2 Absorber Operating Conditions	(TO-02)	(TO-03)
Overhead Pressure	20.9 bar	20.9 bar
Column Pressure Drop	0.1 bar	0.1 bar
2nd Stage SO_2 Absorber Operating Conditions	(TO-03)	(TO-04)
Overhead Pressure	20.8 bar	20.8 bar
Column Pressure Drop	0.1 bar	0.1 bar
H_2O/O_2 Molar Feed Ratio	38	40
SO_2 Stripper Operating Conditions	(TO-04)	(TO-05)
Overhead Pressure	1 bar	1 bar
(Partial-Vapor) Condenser Temperature	48 °C	48 °C
Bottoms Product SO_2 Concentration*	1.8×10^{-3} wt%	1.4×10^{-3} wt%
Column Pressure Drop	0.1 bar	0.1 bar
Electric Power Generation Efficiency (kJ_e/kJ_{th})	48 %	45 %

* Controlled to achieve 1 ppm SO_2 in 2nd Stage SO_2 Absorber overhead product

Table 2 950°C ROT HyS process flowsheet stream table.

Stream	Molar flow rates, kmol/sec*						Temperature,		Pressure,	Phase
ID	H_2O	H_2SO_4	SO_2	O_2	H_2	Total	°C	K	bar	
1	138.00	0	0	0	0.0422	138.04	115.45	388.60	22.750	L
2	21.834	5.7659	2	2E-05	0	29.600	112.59	385.74	22.750	L
3	137.00	0	0	0	1.0422	138.04	120.00	393.15	21.750	L + V
4	0.10347	0	0	0	1	1.1035	120.00	393.15	21.750	V
5	0	0	0	0	1	1	48.00	321.15	20.000	V
6	136.90	0	0	0	0.0422	136.94	120.00	393.15	21.750	L
7	136.90	0	0	0	0.0422	136.94	116.00	389.15	21.000	L + V
8	0.10347	0	0	0	0	0.10347	48.00	321.15	20.000	L
9	1	0	0	0	0	1	40.00	313.15	20.000	L
10	138.00	0	0	0	0.0422	138.04	115.42	388.57	20.000	L + V
11	20.834	6.7659	1	2E-05	0	28.600	120.00	393.15	21.750	L
12	20.834	6.7659	1	2E-05	0	28.600	116.00	389.15	21.000	L
13	3.0821	1.0009	0.14794	2.9E-06	0	4.2309	116.00	389.15	21.000	L
14	3.0821	1.0009	0.14794	2.9E-06	0	4.2309	105.57	378.72	1.013	L + V
15	3.0382	1.0009	0.00863	2.2E-09	0	4.0477	105.57	378.72	1.013	L
16	3.0382	1.0009	0.00863	2.2E-09	0	4.0477	103.47	376.62	0.330	L + V
17	3.0234	1.0009	0.00126	0	0	4.0256	103.47	376.62	0.330	L
18	3.0234	1.0009	0.00126	0	0	4.0256	103.47	376.62	0.430	L
19	3.0234	1.0009	0.00126	0	0	4.0256	103.47	376.62	0.330	L + V
20	3.0234	1.0009	0.00126	0	0	4.0256	115.40	388.55	0.130	L + V
21	3.7568	2.0702	1.5E-08	0	0	5.8270	122.86	396.01	0.130	L
22	3.7568	2.0702	1.5E-08	0	0	5.8270	123.62	396.77	86.000	L
23	4.7577	1.0693	1.0009	0.50046	0	7.3283	254.50	527.65	84.000	L + V
24	4.2803	1.0693	0.22812	0.00805	0	5.5857	254.50	527.65	84.000	L
25	4.2803	1.0693	0.22812	0.00805	0	5.5857	235.12	508.27	22.200	L + V
26	4.0273	1.0693	0.05077	9.8E-05	0	5.1474	235.12	508.27	22.200	L
27	4.0273	1.0693	0.05077	9.8E-05	0	5.1474	187.36	460.51	4.000	L + V
28	3.5270	1.0693	0.00205	1.1E-07	0	4.5983	187.36	460.51	4.000	L
29	3.5270	1.0693	0.00205	1.1E-07	0	4.5983	120.33	393.48	0.330	L + V
30	2.8790	1.0693	9.2E-06	0	0	3.9483	120.33	393.48	0.330	L
31	2.8790	1.0693	9.2E-06	0	0	3.9483	120.33	393.48	0.430	L
32	2.8790	1.0693	9.2E-06	0	0	3.9483	120.33	393.48	0.330	L + V
33	2.8790	1.0693	9.2E-06	0	0	3.9483	125.53	398.68	0.130	L + V
34	0.47738	5.5E-06	0.77280	0.49241	0	1.7426	254.50	527.65	84.000	V
35	0.47738	5.5E-06	0.77280	0.49241	0	1.7426	130.33	403.48	83.400	L + V
36	0.47738	5.5E-06	0.77280	0.49241	0	1.7426	48.00	321.15	82.800	L + V
37	0.47738	5.5E-06	0.77280	0.49241	0	1.7426	30.91	304.06	21.000	L + V
38	0.47566	5.5E-06	0.61477	0.00045	0	1.0909	30.91	304.06	21.000	L
39	0.00172	0	0.15802	0.49195	0	0.65170	30.91	304.06	21.000	V
40	0.25306	1.3E-06	0.17735	0.00795	0	0.43836	235.12	508.27	22.200	V
41	0.25306	1.3E-06	0.17735	0.00795	0	0.43836	130.33	403.48	21.600	L + V
42	0.25306	1.3E-06	0.17735	0.00795	0	0.43836	48.00	321.15	21.000	L + V

43	0.25297	1.3E-06	0.17252	0.00012	0	0.42562	48.00	321.15	21.000	L
44	8.4E-05	0	0.00483	0.00783	0	0.01274	48.00	321.15	21.000	V
45	17.752	5.7650	0.85206	1.7E-05	0	24.369	116.00	389.15	21.000	L
46	21.834	5.7659	2.0000	2E-05	0	29.600	112.57	385.72	21.000	L
47	0.04392	3.1E-09	0.13931	2.9E-06	0	0.18323	105.57	378.72	1.013	V
48	0.50024	8E-07	0.04872	9.8E-05	0	0.54905	187.36	460.51	4.000	V
49	0.50024	8E-07	0.04872	9.8E-05	0	0.54905	130.33	403.48	3.900	L + V
50	0.50024	8E-07	0.04872	9.8E-05	0	0.54905	92.10	365.25	1.013	L + V
51	0.54416	8E-07	0.18803	0.0001	0	0.73229	48.00	321.15	0.913	L + V
52	0.02670	0	0.19038	0.0001	0	0.21718	48.00	321.15	0.913	V
53	0.00495	0	0.30352	0.00623	0	0.31471	48.00	321.15	21.000	L + V
54	0.00494	0	0.29896	6.4E-05	0	0.30397	48.00	321.15	21.000	L
55	0.01944	0	0.39780	6.4E-05	0	0.41731	47.19	320.34	21.000	L
56	0.03498	0	0.00099	2.4E-08	0	0.03597	48.00	321.15	2.501	L
57	0.03498	0	0.00099	2.4E-08	0	0.03597	49.13	322.28	21.000	L
58	0.0145	0	0.09884	3.9E-07	0	0.11334	48.00	321.15	7.308	L
59	0.0145	0	0.09884	3.9E-07	0	0.11334	49.27	322.42	21.000	L
60	1.1E-05	0	0.00456	0.00616	0	0.01074	48.00	321.15	21.000	V
61	0.51849	8E-07	0.005	3.9E-09	0	0.5235	48.00	321.15	0.913	L
62	0.51849	8E-07	0.005	3.9E-09	0	0.5235	48.41	321.56	21.000	L
63	0.01473	9.6E-10	0.00737	2.2E-09	0	0.0221	103.47	376.62	0.330	V
64	0.64799	2.5E-07	0.00204	1.1E-07	0	0.65004	120.33	393.48	0.330	V
65	0.66272	2.5E-07	0.00942	1.2E-07	0	0.67214	43.00	316.15	0.230	L + V
66	0.65796	2.5E-07	0.00151	0	0	0.65947	43.00	316.15	0.230	L
67	0.65796	2.5E-07	0.00151	0	0	0.65947	43.38	316.53	21.000	L
68	0.00497	0	0.00825	1.2E-07	0	0.01323	43.00	316.15	0.230	V
69	0.08905	0	0	0	0	0.08905	169.98	443.13	7.908	L + V
70	0.09402	0	0.00825	1.2E-07	0	0.10228	137.12	410.27	1.013	V
71	0.09299	0	0.0009	0	0	0.09389	48.00	321.15	0.913	L
72	0.09299	0	0.0009	0	0	0.09389	48.00	321.15	1.013	L
73	0.00103	0	0.00736	1.2E-07	0	0.00839	48.00	321.15	0.913	V
74	2.1439	0	0.0009	0	0	2.1448	44.06	317.21	0.110	L
75	2.1439	0	0.0009	0	0	2.1448	44.31	317.46	21.000	L
76	0.00178	0	0.00036	0	0	0.00215	44.06	317.21	0.110	V
77	0.00404	0	0	0	0	0.00404	169.98	443.13	7.908	L + V
78	0.00583	0	0.00036	0	0	0.00619	113.41	386.56	0.330	V
79	0.00562	0	1.3E-05	0	0	0.00563	43.00	316.15	0.230	L
80	0.00562	0	1.3E-05	0	0	0.00563	43.05	316.20	1.013	L
81	0.09861	0	0.00091	0	0	0.09952	47.73	320.88	1.013	L
82	0.00021	0	0.00035	0	0	0.00056	43.00	316.15	0.230	V
83	2.1162	0	0.00089	0	0	2.1170	44.31	317.46	21.000	L
84	3.3445	1.1E-06	0.62765	8E-06	0	3.9722	86.32	359.47	21.000	L
85	0.01835	6.5E-10	0.66481	0.00065	0	0.68381	112.57	385.72	21.000	V
86	0.00836	0	0.21303	0.50659	0	0.72798	59.80	332.95	20.900	V
87	0.02773	0	1.2E-05	0	0	0.02775	44.31	317.46	21.000	L
88	19	0	0.00011	0	0	19.000	48.00	321.15	21.000	L

89	19.005	0	0.21313	0.00613	0	19.224	51.93	325.08	20.900	L
90	0.00514	0	5.8E-05	1.7E-06	0	0.0052	51.93	325.08	20.900	L
91	19	0	0.21307	0.00613	0	19.219	51.93	325.08	20.900	L
92	19	0	0.21307	0.00613	0	19.219	52.11	325.26	1.800	L + V
93	19	0	0.21307	0.00613	0	19.219	82.29	355.44	1.050	L + V
94	18.972	0	9.4E-05	0	0	18.972	99.63	372.78	1.100	L
95	18.972	0	9.4E-05	0	0	18.972	99.86	373.01	22.500	L
96	18.972	0	9.4E-05	0	0	18.972	62.11	335.26	21.750	L
97	18.972	0	9.4E-05	0	0	18.972	48.00	321.15	21.000	L
98	0.02773	0	0.21297	0.00613	0	0.24683	48.00	321.15	1.000	V
99	0.00323	0	5E-07	0.50046	0	0.50368	48.04	321.19	20.800	V
100	0	0	0	0.50046	0	0.50046	48.00	321.15	19.800	V
101	0.00323	0	5E-07	0	0	0.00323	48.00	321.15	19.800	L
102	0.00323	0	5E-07	0	0	0.00323	48.07	321.22	21.000	L
BFW	0.09309	0	0	0	0	0.09309	38.00	311.15	1.000	L
MAKEUP	0.0046	0.00091	0	0	0	0.00552	38.00	311.15	21.000	L
STEAM	0.09309	0	0	0	0	0.09309	170.07	443.22	7.908	V

* Individual component molar flow rates < $1x10^{-9}$ kmol/sec are shown as zero.

Table 3 950°C ROT HyS process flowsheet energy utilization summary.

Electric power requirements:		
EL-01, Electrolyzer	115.782	MW_e
CO-01, SO_2 Recycle Compressor		
Stage 1	1.986	MW_e
Stage 2	1.869	MW_e
Stage 3	1.254	MW_e
PP-01, Catholyte Feed Pump	0.842	MW_e
PP-02, Vacuum Column Feed Pump	0.001	MW_e
PP-03, Bayonet Reactor Feed Pump	1.830	MW_e
PP-04, Vacuum Column Recycle Pump	0.001	MW_e
PP-05, Anolyte Feed Pump	0.155	MW_e
PP-06, First Stage Intercooler Condensate Pump	0.004	MW_e
PP-07, Second Stage Intercooler Condensate Pump	0.012	MW_e
PP-08, First Flash Stage Vapor Condensate Pump	0.033	MW_e
PP-09, Second Flash Stage Vapor Condensate Pump	0.041	MW_e
PP-10, First Stage Ejector Condensate Pump	0.000	MW_e
PP-11, Vacuum Column Distillate Pump	0.111	MW_e
PP-12, Second Stage Ejector Condensate Pump	0.000	MW_e
PP-13, SO_2 Stripper Bottoms Pump	0.888	MW_e
PP-14, O_2 Dryer Liquids Pump	0.000	MW_e
Total electric power requirement:	124.811	MW_e
Heat recuperation summary:		
EX-01, Catholyte Interchanger (EX-01-HS/EX-CS-01, Q1)	42.019	MW_{th}
EX-02, Anolyte Interchanger (EX-02-HS/EX-CS-01, Q2)	11.583	MW_{th}
Bayonet Vapor Product Interchangers		
Stage 1, EX-03 (EX-03-HS/EX-CS-02, Q3)	24.766	MW_{th}
Stage 2, EX-04 (EX-04-HS/EX-CS-02, Q4)	10.586	MW_{th}
Stage 3, EX-05 (EX-05-HS/EX-CS-02, Q5)	16.340	MW_{th}
EX-06, SO_2 Stripper Feed Interchanger	54.136	MW_{th}
Cooling water requirements:		
CO-01 -- SO_2 Recycle Compressor Intercoolers		
Stage 1	3.570	MW_{th}
Stage 2	4.704	MW_{th}
Stage 3	7.991	MW_{th}
DR-01, Hydrogen Dryer	6.774	MW_{th}
DR-02, Oxygen Dryer	0.131	MW_{th}
HX-01, Bayonet Product First Stage Flash Condenser	20.141	MW_{th}
HX-02, Bayonet Product Second Stage Flash Condenser	6.598	MW_{th}
HX-03, First Acid Flash Stage Condenser	9.066	MW_{th}
HX-04, Second Acid Flash Stage Condenser	30.256	MW_{th}
HX-05, First Stage Ejector Condenser	4.187	MW_{th}
HX-06, Second Stage Ejector Condenser	0.258	MW_{th}

HX-07, Second Stage SO_2 Absorber Feed Cooler	20.184	MW_{th}
TO-01 Vacuum Column Condenser	96.383	MW_{th}
TO-04 SO_2 Stripper Condenser	15.891	MW_{th}
Total cooling water requirement:	226.133	MW_{th}
High-temperature heat requirements:		
Secondary helium supply temperature	900.0	°C
Minimum helium return temperature (utility pinch)	514.4	°C
Bayonet Reactor high-temperature heat duty:	340.245	MW_{th}
Low-temperature steam heat requirements:		
Vacuum Ejector Steam Feed (100-psig)	4.376	MW_{th}
TO-01 Vacuum Column Reboiler (30-psig)	5.967	MW_{th}
TO-04 SO2 Stripper Reboiler (10-psig)	39.981	MW_{th}
Total low-pressure steam requirement:	50.324	MW_{th}
Power conversion efficiency (kJ_e/kJ_{th})	48%	
Thermal equivalent of total electric power requirement	260.023	MW_{th}
High-temperature (HTGR) heat requirement	340.245	MW_{th}
Low-temperature (low-pressure steam) heat requirement	50.324	MW_{th}
Total heat requirement:	650.592	MW_{th}
Total heat requirement (excluding low-pressure steam)*:	600.268	MW_{th}
Higher heating value of Hydrogen	286	MJ/kmol H_2
Hydrogen production rate	1	kmol/sec
Equivalent energy content of Hydrogen product	286	MW_{th}

HHV efficiency upper limit, free steam*	47.6%
HHV efficiency upper limit	44.0%

* Assumes that excess 10- to 100-psig steam is available on-site at no penalty

Table 4 750°C ROT HyS process flowsheet stream table.

Stream	Molar flow rates, kmol/sec*						Temperature,		Pressure,	Phase
ID	H_2O	H_2SO_4	SO_2	O_2	H_2	Total	°C	K	bar	
1	137.20	0	0	0	0.04195	137.24	115.45	388.60	22.750	L
2	21.834	5.7659	2	4.9E-05	0	29.600	112.50	385.65	22.750	L
3	136.20	0	0	0	1.0420	137.24	120.00	393.15	21.750	L + V
4	0.10347	0	0	0	1	1.1035	120.00	393.15	21.750	V
5	0	0	0	0	1	1	48.00	321.15	20.000	V
6	136.09	0	0	0	0.04195	136.13	120.00	393.15	21.750	L
7	136.09	0	0	0	0.04195	136.13	116.00	389.15	21.000	L + V
8	0.10347	0	0	0	0	0.10347	48.00	321.15	20.000	L
9	1	0	0	0	0	1	40.00	313.15	20.000	L
10	137.20	0	0	0	0.04195	137.24	115.42	388.57	20.000	L + V
11	20.834	6.7659	1	4.9E-05	0	28.600	120.00	393.15	21.750	L
12	20.834	6.7659	1	4.9E-05	0	28.600	116.00	389.15	21.000	L
13	3.0796	1.0001	0.14782	7.2E-06	0	4.2276	116.00	389.15	21.000	L
14	3.0796	1.0001	0.14782	7.2E-06	0	4.2276	105.57	378.72	1.013	L + V
15	3.0357	1.0001	0.00862	5.5E-09	0	4.0445	105.57	378.72	1.013	L
16	3.0357	1.0001	0.00862	5.5E-09	0	4.0445	103.47	376.62	0.330	L + V
17	3.0210	1.0001	0.00125	0	0	4.0224	103.47	376.62	0.330	L
18	3.0210	1.0001	0.00125	0	0	4.0224	103.47	376.62	0.430	L
19	3.0210	1.0001	0.00125	0	0	4.0224	103.47	376.62	0.330	L + V
20	3.0210	1.0001	0.00125	0	0	4.0224	115.29	388.44	0.130	L + V
21	0.6050	1.0001	0	0	0	1.6051	188.36	461.51	0.130	L
22	0.6050	1.0001	0	0	0	1.6051	188.71	461.86	11.100	L
23	5.8682	3.4292	0.02148	0.00113	0	9.3200	256.78	529.93	11.100	L
24	5.8682	3.4292	0.02148	0.00113	0	9.3200	256.88	530.03	12.700	L
25	6.8682	2.4292	1.02147	0.50113	0	10.820	287.73	560.88	11.700	L + V
26	6.8682	2.4292	1.0215	0.50113	0	10.820	245.69	518.84	11.100	L + V
27	1.6050	0.00013	1	0.5	0	3.1051	235.00	508.15	11.100	V
28	1.6050	0.00013	1	0.5	0	3.1051	142.37	415.52	10.500	L + V
29	1.6050	0.00013	1	0.5	0	3.1051	48.00	321.15	9.900	L + V
30	0.01718	0.00000	0.86680	0.49987	0	1.3838	48.00	321.15	9.900	V
31	0.01718	0.00000	0.86680	0.49987	0	1.3838	130.20	403.35	21.100	V
32	0.01718	0.00000	0.86680	0.49987	0	1.3838	48.00	321.15	21.000	L + V
33	0.00157	0.00000	0.36103	0.49975	0	0.86235	48.00	321.15	21.000	V
34	0.01561	0.00000	0.50577	0.00011	0	0.52149	48.00	321.15	21.000	L
35	1.5878	0.00013	0.13320	0.00013	0	1.7213	48.00	321.15	9.900	L
36	1.5878	0.00013	0.13320	0.00013	0	1.7213	48.16	321.31	21.000	L
37	17.754	5.7658	0.85218	4.1E-05	0	24.372	116.00	389.15	21.000	L
38	21.833	5.7668	1.9991	4.9E-05	0	29.599	112.49	385.64	21.000	L
39	0.04389	3.1E-09	0.13920	7.2E-06	0	0.18309	105.57	378.72	1.013	V
40	0.04389	3.1E-09	0.13920	7.2E-06	0	0.18309	48.00	321.15	0.913	L + V
41	0.02044	0	0.14581	7.2E-06	0	0.16625	48.00	321.15	0.913	V
42	0.00664	0	0.43063	0.00610	0	0.44337	48.00	321.15	21.000	L + V

43	0.00663	0	0.42617	9.1E-05	0	0.43290	48.00	321.15	21.000	L
44	0.02847	0	0.58781	9.1E-05	0	0.61638	47.24	320.39	21.000	L
45	0.04941	0	0.00141	2.3E-08	0	0.05082	48.00	321.15	2.501	L
46	0.04941	0	0.00141	2.3E-08	0	0.05082	49.13	322.28	21.000	L
47	0.02184	0.0000	0.16164	4.3E-07	0	0.18348	48.00	321.15	7.308	L
48	0.02184	0.0000	0.16164	4.3E-07	0	0.18348	49.08	322.23	21.000	L
49	9.9E-06	0	0.00445	0.00601	0	0.01047	48.00	321.15	21.000	V
50	0.02441	3.1E-09	0.00024	0	0	0.02465	48.00	321.15	0.913	L
51	0.02441	3.1E-09	0.00024	0	0	0.02465	49.22	322.37	21.000	L
52	0.01472	9.6E-10	0.00737	5.5E-09	0	0.02208	103.47	376.62	0.330	V
53	0.01472	9.6E-10	0.00737	5.5E-09	0	0.02208	43.00	316.15	0.230	L + V
54	0.01029	9.6E-10	2.4E-05	0	0	0.01031	43.00	316.15	0.230	L
55	0.01029	9.6E-10	2.4E-05	0	0	0.01031	44.25	317.40	21.000	L
56	0.00463	0	0.00768	5.5E-09	0	0.01231	43.00	316.15	0.230	V
57	0.08289	0	0.00000	0	0	0.08289	169.98	443.13	7.908	L + V
58	0.08752	0	0.00768	5.5E-09	0	0.09520	137.12	410.27	1.013	V
59	0.08656	0	0.00084	0	0	0.08740	48.00	321.15	0.913	L
60	0.08656	0	0.00084	0	0	0.08740	48.01	321.16	1.013	L
61	0.00096	0	0.00685	5.5E-09	0	0.00781	48.00	321.15	0.913	V
62	2.4140	0	0.00090	0	0	2.4149	44.57	317.72	0.110	L
63	2.4140	0	0.00090	0	0	2.4149	44.81	317.96	21.000	L
64	0.00206	0	0.00036	0	0	0.00242	44.57	317.72	0.110	V
65	0.00446	0	0	0	0	0.00446	169.98	443.13	7.908	L + V
66	0.00652	0	0.00036	0	0	0.00688	113.21	386.36	0.330	V
67	0.00631	0	1.5E-05	0	0	0.00633	43.00	316.15	0.230	L
68	0.00631	0	1.5E-05	0	0	0.00633	43.05	316.20	1.013	L
69	0.09288	0	0.00085	0	0	0.09373	47.68	320.83	1.013	L
70	0.00021	0	0.00034	0	0	0.00055	43.00	316.15	0.230	V
71	2.3565	0	0.00088	0	0	2.3574	44.81	317.96	21.000	L
72	2.4481	4.4E-09	0.24974	0.00046	0	2.6983	68.67	341.82	21.000	L
73	0.00908	3.2E-10	0.32955	0.00079	0	0.33942	112.49	385.64	21.000	V
74	0.01532	0	0.44811	0.50610	0	0.96953	66.64	339.79	20.900	V
75	0.05746	0	2.1E-05	0	0	0.05748	44.81	317.96	21.000	L
76	20.000	0	0.00010	0	0	20.000	48.00	321.15	21.000	L
77	20.012	0	0.44821	0.00610	0	20.466	55.37	328.52	20.900	L
78	0.0121	0	0.00027	3.7E-06	0	0.01237	55.37	328.52	20.900	L
79	20	0	0.44794	0.00609	0	20.454	55.37	328.52	20.900	L
80	20	0	0.44794	0.00609	0	20.454	53.60	326.75	1.800	L + V
81	20	0	0.44794	0.00609	0	20.454	79.69	352.84	1.050	L + V
82	19.943	0	7.9E-05	0	0	19.943	102.31	375.46	1.100	L
83	19.943	0	7.9E-05	0	0	19.943	102.55	375.70	22.500	L
84	19.943	0	7.9E-05	0	0	19.943	63.60	336.75	21.750	L
85	19.943	0	7.9E-05	0	0	19.943	48.00	321.15	21.000	L
86	0.05746	0	0.44786	0.00609	0	0.51141	48.00	321.15	1.000	L + V
87	0.00322	0	5E-07	0.5	0	0.50322	48.04	321.19	20.800	V
88	0	0	0	0.5	0	0.5	48.04	321.19	19.800	V

89	0.00322	0	5E-07	0	0	0.00322	48.04	321.19	19.800	L
90	0.00322	0	5E-07	0	0	0.00322	48.11	321.26	21.000	L
BFW	0.08735	0	0	0	0	0.08735	38.00	311.15	1.000	L
MAKEUP	0.00468	0.00085	0	0	0	0.00553	38.00	311.15	21.000	L
STEAM	0.08735	0	0	0	0	0.08735	170.08	443.23	7.910	V
DT1						2.9636†	120.00	393.15	2.000	L
DT2						2.9636†	120.13	393.28	6.500	L
DT3						2.9636†	153.84	426.99	5.750	L
DT4						2.9636†	156.38	429.53	5.000	L
DT5						2.9636†	250.00	523.15	4.250	L
DT6						2.9636†	246.91	520.06	3.500	L
DT7						2.9636†	164.43	437.58	2.750	L

* Individual component molar flow rates < $1x10^{-9}$ kmol/sec are shown as zero.

† Molar flow rate of DOWTHERM G, kmol/sec.

Table 5 750°C ROT HyS process flowsheet energy utilization summary.

Electric power requirements:		
EL-01, Electrolyzer	115.782	MW_e
CO-01, SO_2 Recycle Compressor		
Stage 1	2.900	MW_e
Stage 2	2.736	MW_e
Stage 3	1.765	MW_e
CO-02, SO_2/O_2 Compressor	3.983	MW_e
PP-01, Catholyte Feed Pump	0.837	MW_e
PP-02, Vacuum Column Feed Pump	0.001	MW_e
PP-03, Quench Column Feed Pump	0.096	MW_e
PP-04, Bayonet Reactor Feed Pump	0.067	MW_e
PP-05, Quench Column Overhead Condensate Pump	0.052	MW_e
PP-06, Anolyte Feed Pump	0.155	MW_e
PP-07, First Stage Intercooler Condensate Pump	0.006	MW_e
PP-08, Second Stage Intercooler Condensate Pump	0.017	MW_e
PP-09, First Flash Stage Vapor Condensate Pump	0.003	MW_e
PP-10, Second Flash Stage Vapor Condensate Pump	0.001	MW_e
PP-11, First Stage Ejector Condensate Pump	0.000	MW_e
PP-12, Vacuum Column Distillate Pump	0.124	MW_e
PP-13, Second Stage Ejector Condensate Pump	0.000	MW_e
PP-14, SO_2 Stripper Bottoms Pump	0.935	MW_e
PP-15, O_2 Dryer Liquids Pump	0.000	MW_e
PP-16, Dowtherm Pump	0.332	MW_e
Total electric power requirement:	129.795	MW_e
Heat recuperation summary:		
EX-01, Catholyte Interchanger (EX-01-HS/EX-CS-01, Q1)	41.772	MW_{th}
EX-02, Anolyte Interchanger (EX-02-HS/EX-CS-01, Q2)	11.583	MW_{th}
EX-03, SO_2 Stripper Feed Interchanger	58.748	MW_{th}
Cooling water requirements:		
CO-01 -- SO_2 Recycle Compressor Intercoolers		
Stage 1	5.139	MW_{th}
Stage 2	7.277	MW_{th}
Stage 3	11.354	MW_{th}
DR-01, Hydrogen Dryer	6.774	MW_{th}
DR-02, Oxygen Dryer	0.131	MW_{th}
HX-03, Quench Column Overhead Cooler	55.332	MW_{th}
HX-04, SO_2/O_2 Compressor Effluent Cooler	15.818	MW_{th}
HX-05, First Acid Flash Stage Condenser	1.478	MW_{th}
HX-06, Second Acid Flash Stage Condenser	0.494	MW_{th}
HX-07, First Stage Ejector Condenser	3.902	MW_{th}
HX-08, Second Stage Ejector Condenser	0.290	MW_{th}
HX-09, Second Stage SO_2 Absorber Feed Cooler	23.450	MW_{th}

TO-01 Vacuum Column Condenser	115.140	MW_{th}
TO-02 Quench Column Condenser	2.861	MW_{th}
TO-04 SO_2 Stripper Condenser	24.644	MW_{th}
Total cooling water requirement:	274.084	MW_{th}
Intermediate temperature heat sources:		
HX-01, Bayonet Reactor Effluent Cooler	115.571	MW_{th}
Inlet Temperature:	287.7	°C
Outlet Temperature:	245.7	°C
TO-02 Quench Column Condenser	2.861	MW_{th}
Inlet Temperature:	256.8	°C
Outlet Temperature:	235.0	°C
HX-02, Quench Column Overhead Cooler	37.010	MW_{th}
Inlet Temperature:	234.4	°C
Outlet Temperature:	142.4	°C
Total intermediate temperature heat sources:	155.443	MW_{th}
Intermediate temperature heat sinks:		
TO-01 Vacuum Column Reboiler	102.309	MW_{th}
Inlet Temperature:	114.8	°C
Outlet Temperature:	188.4	°C
TO-05 SO_2 Stripper Reboiler	49.027	MW_{th}
Inlet Temperature:	101.9	°C
Outlet Temperature:	102.3	°C
SG-01, Steam Generator	4.106	MW_{th}
Inlet Temperature:	37.9	°C
Outlet Temperature:	170.1	°C
Total intermediate temperature heat sinks:	155.443	MW_{th}
High-temperature heat requirements:		
Secondary helium supply temperature	700.0	°C
Minimum helium return temperature (utility pinch)	425.5	°C
Bayonet Reactor high-temperature heat duty:	428.291	MW_{th}
Power conversion efficiency (kJ_e/kJ_{th})	45%	
Thermal equivalent of total electric power requirement	288.433	MW_{th}
High-temperature (HTGR) heat requirement	428.291	MW_{th}
Total heat requirement:	716.724	MW_{th}
Higher heating value of Hydrogen	286	MJ/kmol H_2
Hydrogen production rate	1	kmol/sec
Equivalent energy content of Hydrogen product	286	MW_{th}
HHV efficiency upper limit	39.9%	